Supplementary Table 1: Characteristics of spontaneous Ptch;p53 MBs used in the study									
subtype	mice ID	Ptch;p53	gender	latency	# cells injected	Tumor take rate		control	LDE
SI-CSC	x16650	het:hom	M	60	2X10^6	18/20	90%	6/6	5/5
SI-CSC	x17282	het;hom	M	50	3X10^6	18/20	90%	6/6	6/6
SD-CSC I	x15924	het:het	F	145	3X10^6	5/10	50%	4/4	1/1
SD-CSC I	F3572 (2' of x15924)	het;het			2X10^6	9/20	45%	2/2	0/2
SD-CSC I	x15811	het;wt	M	181	3X10^6	5/10	50%	2/4	0/1
SD-CSC I	F3590 (2' of x15811)	het;wt			2X10^6	7/20	35%	1/2	0/3
SD-CSC I	x15762	het;het	F	218	3X10^6	6/10	60%	3/3	0/3
SD-CSC I	x16660	het;wt	F	216	3.8X10^6	14/16	88%	4/4	4/4
SD-CSC I	x16598	het;wt	F	242	3.5X10^6	11/16	69%	3/3	3/3
SD-CSC I	x16934	het;het	F	193	2X10^6	12/20	60%	1/1	3/3
SD-CSC II	F4479	het;hom	M	65	4X10^6	11/20	55%	3/3	3/3
SD-CSC II	x16192	het;het	F	221	1X10^6	8/20	40%	3/3	3/3

Supplementary Table 2: Bisulfide sequencing sample information				
Sample ID	Source	Tumor Type	Cell line	Treatment
LPMeseq1	918 parental	SD-CSC	918	none
LPMeseq2	918 DMSO	SD-CSC	918	DMSO
LPMeseq3	918 LDEr	SD-CSC	918	LDE
LPMeseq4	2869 DMSO	SD-CSC	2869	DMSO
LPMeseq5	2869 LDEr	SD-CSC	2869	LDE
LPMeseq6	17282 parental	SI-CSC	17282	none
LPMeseq7	17282 DMSO	SI-CSC	17282	DMSO
LPMeseq8	17282 LDEr	SI-CSC	17282	LDE
LPMeseq9	9410 DMSO	SI-CSC	9410	DMSO
LPMeseq10	9410 LDEr	SI-CSC	9410	LDE

Supp Fig1

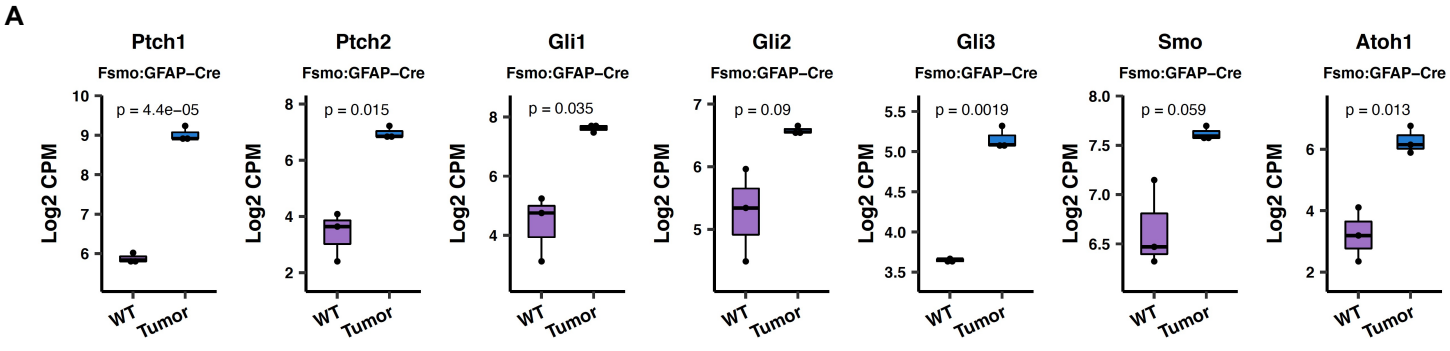
A
Ptch1
Ptch2
Gli1
Gli2
Gli3
Smo
Atoh1
Fsmo:GFAP–Cre
Log2 CPM
p = 4.4e–05
p = 0.015
p = 0.035
p = 0.09
p = 0.0019
p = 0.059
p = 0.013
WT
Tumor

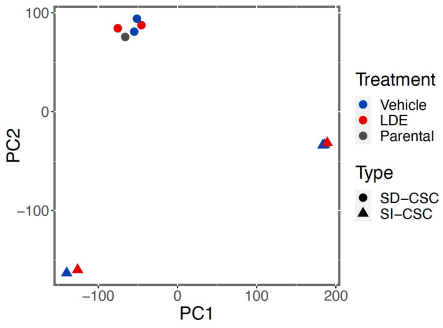
B
PC1
PC2
Treatment
Vehicle
LDE
Parental
Type
SD–CSC
SI–CSC

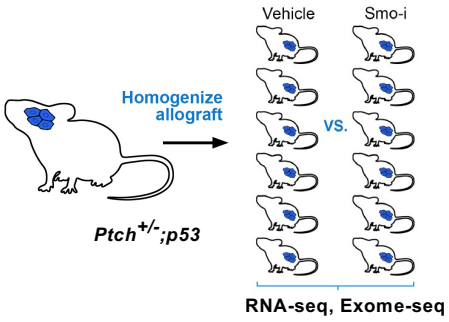
C
Homogenize allograft
Ptch+/-;p53
Vehicle
Smo-i
VS.
RNA-seq, Exome-seq

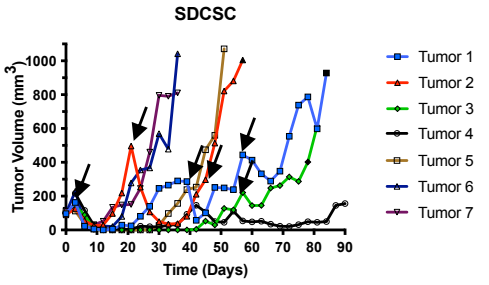
D
SDCSC
Tumor Volume (mm3)
Time (Days)
Tumor 1
Tumor 2
Tumor 3
Tumor 4
Tumor 5
Tumor 6
Tumor 7

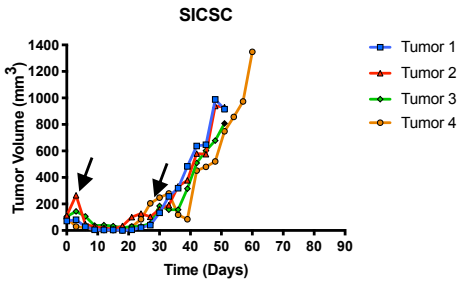
SICSC
Tumor Volume (mm3)
Time (Days)
Tumor 1
Tumor 2
Tumor 3
Tumor 4

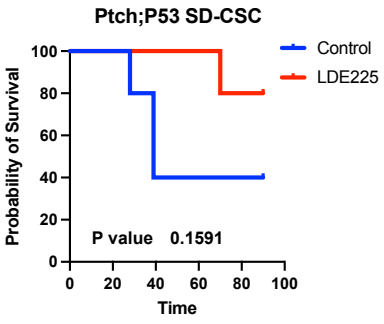
E
Ptch;P53 SD-CSC
Probability of Survival
Time
Control
LDE225
P value 0.1591

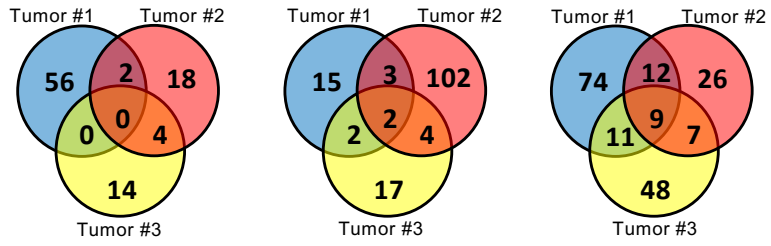
F
Tumor #1
Tumor #2
Tumor #3
56
2
18
0
4
14
15
3
102
2
4
17
74
12
26
9
11
7
48

G

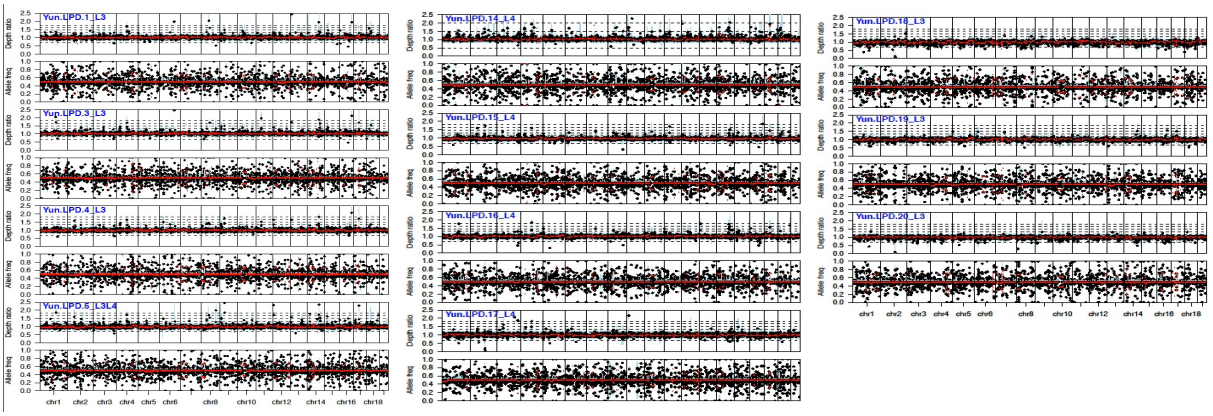

H

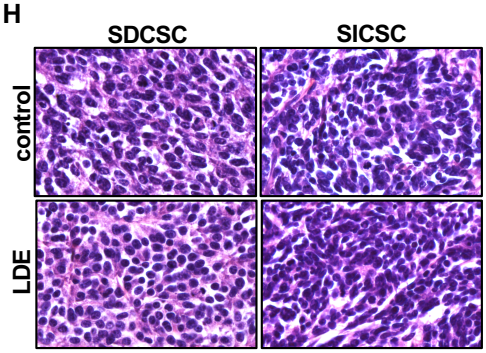

I

Sample	Moderate + High Impact	High Impact
Yun.LPD_LDE.14_L4	10	0
Yun.LPD_LDE.15_L4	26	2
Yun.LPD_LDE.16_L4	7	0
Yun.LPD_LDE.17_L4	12	2
Yun.LPD_LDE.18_L3	6	1
Yun.LPD_LDE.19_L3	7	1
Yun.LPD_LDE.20_L3	8	4
Yun.LPD_Vehicle.1_L3	21	1
Yun.LPD_Vehicle.3_L3	21	2
Yun.LPD_Vehicle.4_L3	10	3
Yun.LPD_Vehicle.5_L3L4	25	3

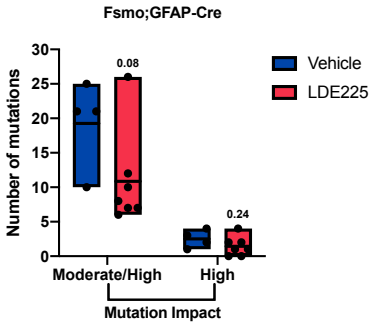

Supplementary Figure 1. ***FsmoM2;hGFAP-cre*** **and** ***Ptch;p53*** **SHH MB models treated with LDE225. A**) Elevated SHH signaling pathway genes in *FsmoM2;hGFAP-Cre MB* compared to wildtype cerebellum at p8. Box represents log_2-scaled CPM range in RNA-seq data. Central line represents the mean. P-values were calculated using two-tailed Student's t-test. **B)** Whole-genome methylation profiles depict significant differences between SI-CSC and SD-CSCs. The dimensionality of methylation profiles of all the samples was reduced using Principal Component Analysis (PCA). A scatter plot on the two-dimensional plane using the first two principal components shows the significant differences between SD-CSCs and SI-CSCs. **C)** A schematic outlining experimental design: spontaneous *Ptch;p53* MBs tumor tissues were isolated, diced into small pieces, and admixed before injecting into a cohort of recipient mice that were randomly divided into two groups (vehicle vs. LDE225(SMOi) treatment). **D)** Representative growth profiles of SD-CSC and SI-CSC tumors treated with LDE225. **E**) Kaplan-Meier survival curve analysis showing survival difference between vehicle and LDE225 treated *Ptch:p53* SD-CSC tumors. **F)** Venn diagrams showing the number of treatment-induced SNPs in each subtype and their overlaps. Numbers indicate SNPs present in LDE-resistant tumors and absent in control-treated tumors from the matching parental tumor. See supplementary tables 3 and 4. **G**) A summary of identified mutations and copy number alterations in the SHH pathway genes in SMOi-resistant *Ptch:p53* SI-CSC and SD-CSC tumors. **H**) H&E staining of control and LDE225 treated tumors at harvest. N=3. **I**) Moderate and high impact mutations identified in vehicle and LDE225 treated *FsmoM2;hGFAP-Cre MB* MB, compared to normal tail DNA by whole exome sequencing analysis. Also see Supp Table 5.

SuppFig2

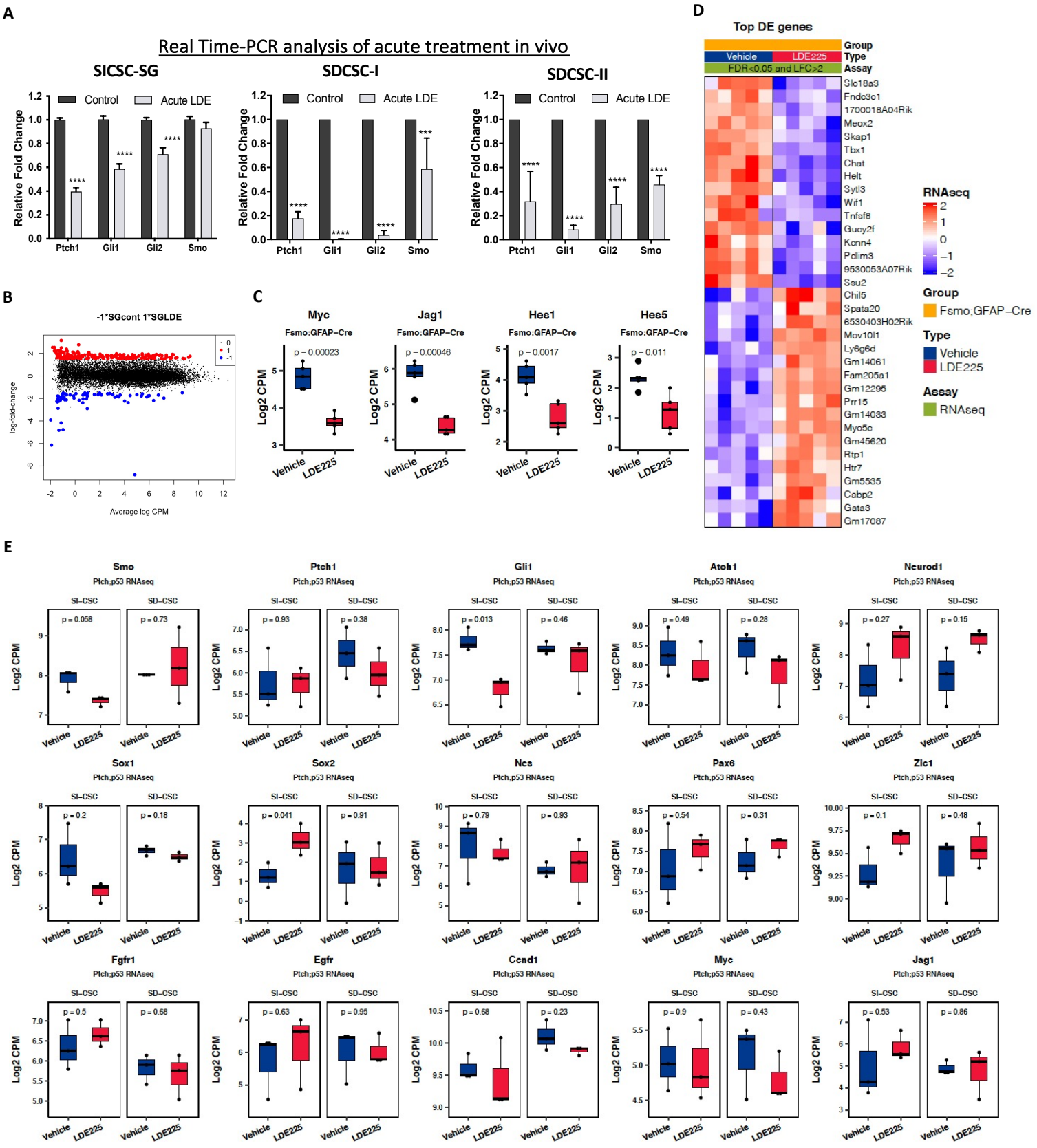
A
Real Time-PCR analysis of acute treatment in vivo
SICSC-SG
SDCSC-I
SDCSC-II
Control
Acute LDE
Relative Fold Change
Ptch1
Gli1
Gli2
Smo
B
-1*SGcont 1*SGLDE
log-fold-change
Average log CPM
C
Myc
Jag1
Hes1
Hes5
Fsmo:GFAP−Cre
Log2 CPM
Vehicle
LDE225
D
Top DE genes
Group
Type
Assay
FDR<0.05 and LFC>2
RNAseq
Group
Fsmo;GFAP−Cre
Type
Vehicle
LDE225
Assay
RNAseq
E
Smo
Ptch1
Gli1
Atoh1
Neurod1
Sox1
Sox2
Ncs
Pax6
Zic1
Fgfr1
Egfr
Ccnd1
Myc
Jag1
Ptch;p53 RNAseq
SI−CSC
SD−CSC

SuppFig2 Cont.

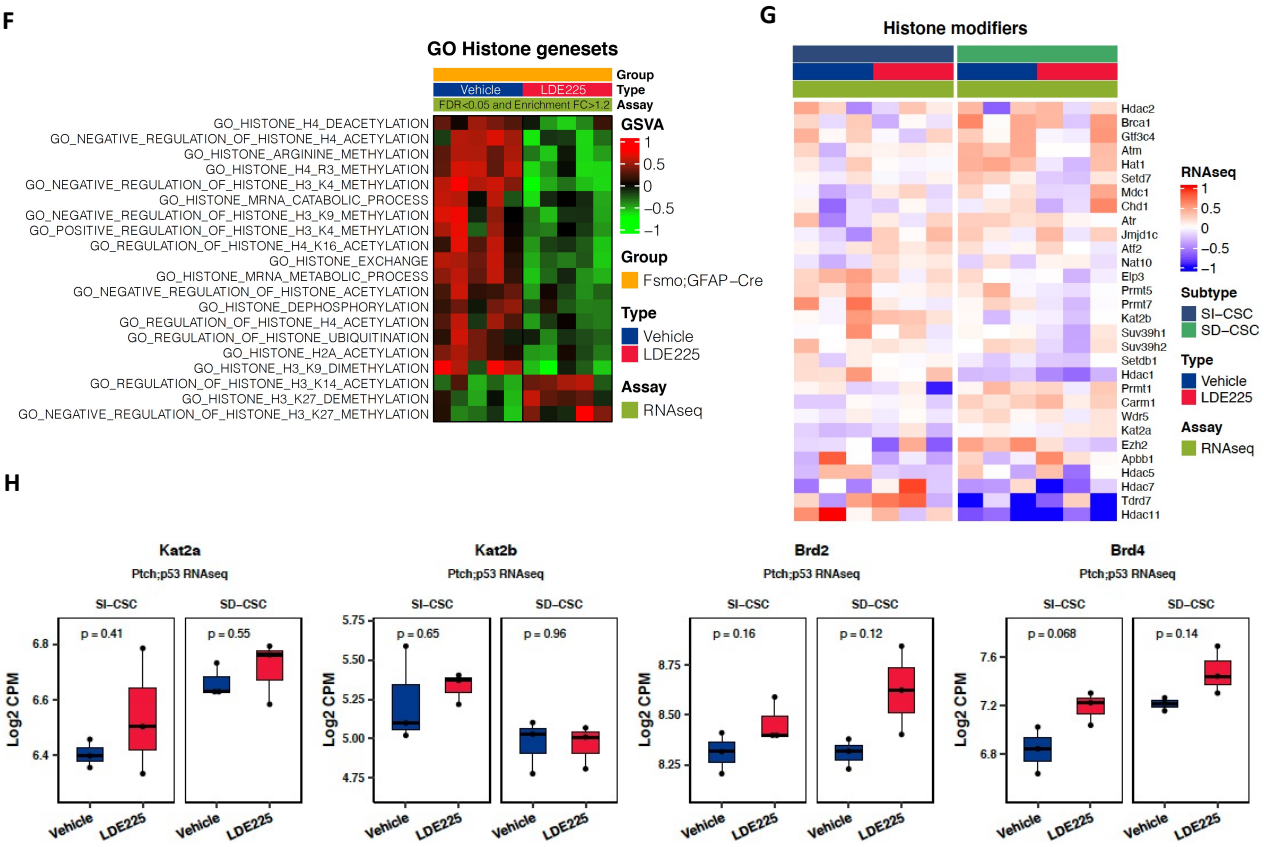

Supplementary Figure 2. Acute and long-term LDE225 treatment reduce SHH , Notch signaling and histone modification gene expression. A) RT-PCR analyses showing on-target response (reduced *Ptch1, Gli1, Gli2, and Smo* RNA levels) in all tumors, regardless of subtype, to acute (2 day) treatment with LDE225. Relative expression levels are normalized to control treated sister allografts. P-values were calculated using ordinary one-way ANOVA with Sidak's multiple comparisons test. N=3, ****P < 0.0001, ***P<0.001. **B**) Mean-difference plot showing RNA-seq expression data of 5 control-treated and 5 LDE225-treated *FSmoM2;hGFAP-Cre MB*. **C**) Expression levels of Myc and Notch pathway genes in vehicle vs. LDE225-treated *FSmoM2;hGFAP-Cre* SI-CSC *MB*s. Box represents $\log_2$-scaled CPM range. Central line represents the mean. P-values were calculated using two-tailed Student's t-test. **D**) Top differentially expressed genes from vehicle vs LDE225 treated *FSmoM2;hGFAP-Cre MB* are represented as Log2-scaled CPM RNA-seq in a heatmap. Each column represents an independent tumor. **E**) Expression levels of *SHH,* neuronal stem cell and differentiation markers in vehicle vs. LDE225-treated *Ptch;P53* MBs. Box represents $\log_2$-scaled CPM range in RNA-seq data. Central line represents the mean. P-values were calculated using two-tailed Student's t-test. . **F**) GSVA analyses (GSVA enrichment score FC>1.2 and p-value <0.05) of vehicle vs. LDE225-treated *FSmoM2;hGFAP-Cre* SI-CSC MBs showing differential enrichment of histone modification gene sets. **G**) heatmap showing histone modification-related genes in *Ptch;P53* SD-CSC MBs. FDR <0.05 and log fold change>2. **H**) Expression levels of *Kat2a, Kat2b, Brd2 and Brd4* in Vehicle vs. LDE225-treated *Ptch;P53* SD-CSC MBs. Box represents $\log_2$-scaled CPM range in RNA-seq data. Central line represents the mean. P-values were calculated using two-tailed Student's t-test.

SuppFig3

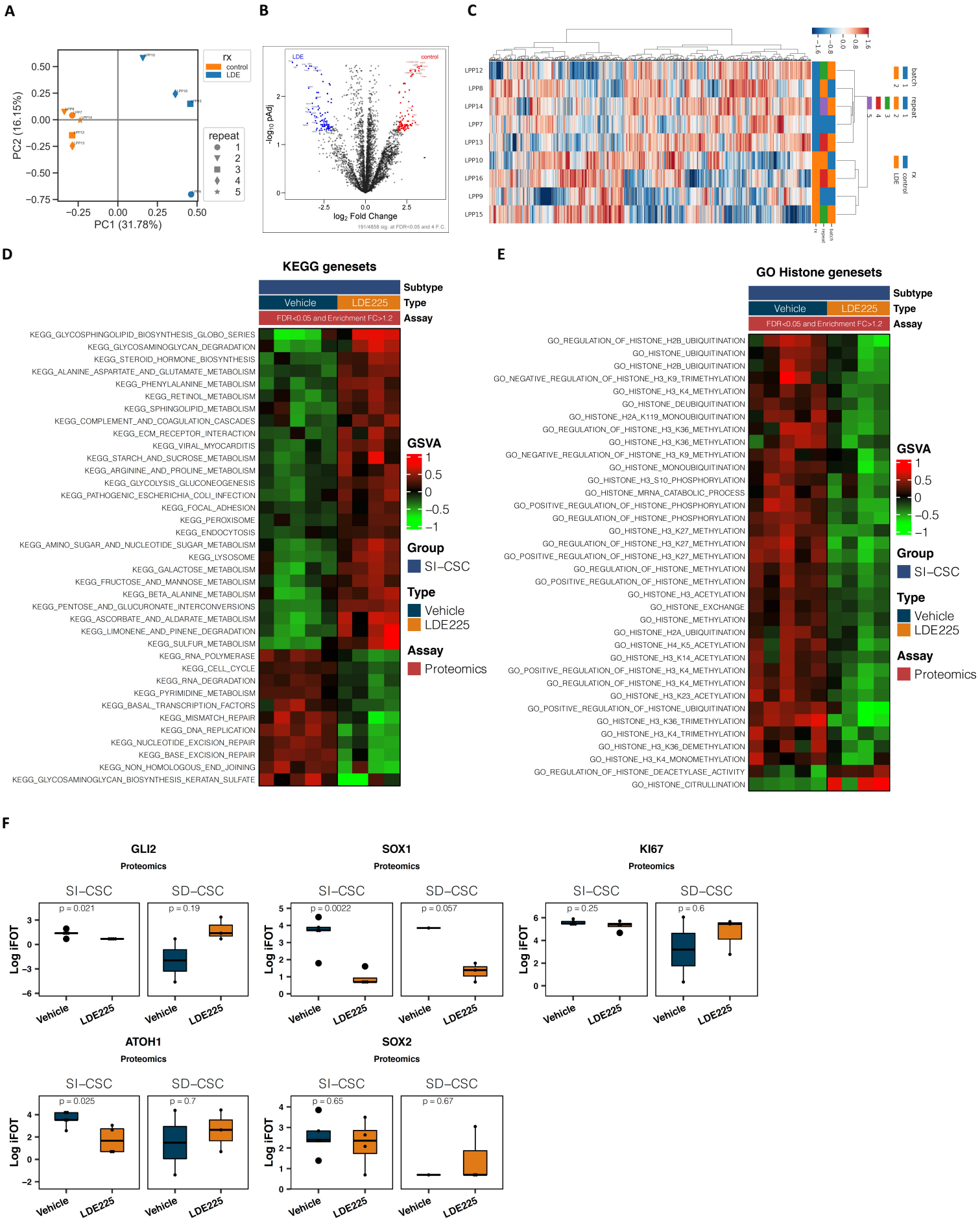
A
PC2 (16.15%)
PC1 (31.78%)
rx
control
LDE
repeat
1
2
3
4
5
B
LDE
control
-log10 pAdj
log2 Fold Change
191/4858 sig. at FDR<0.05 and 4 F.C.
C
LPP12
LPP8
LPP14
LPP7
LPP13
LPP10
LPP16
LPP9
LPP15
batch
repeat
rx
control
LDE
D
KEGG genesets
Subtype
Vehicle
LDE225
Type
FDR<0.05 and Enrichment FC>1.2
Assay
KEGG_GLYCOSPHINGOLIPID_BIOSYNTHESIS_GLOBO_SERIES
KEGG_GLYCOSAMINOGLYCAN_DEGRADATION
KEGG_STEROID_HORMONE_BIOSYNTHESIS
KEGG_ALANINE_ASPARTATE_AND_GLUTAMATE_METABOLISM
KEGG_PHENYLALANINE_METABOLISM
KEGG_RETINOL_METABOLISM
KEGG_SPHINGOLIPID_METABOLISM
KEGG_COMPLEMENT_AND_COAGULATION_CASCADES
KEGG_ECM_RECEPTOR_INTERACTION
KEGG_VIRAL_MYOCARDITIS
KEGG_STARCH_AND_SUCROSE_METABOLISM
KEGG_ARGININE_AND_PROLINE_METABOLISM
KEGG_GLYCOLYSIS_GLUCONEOGENESIS
KEGG_PATHOGENIC_ESCHERICHIA_COLI_INFECTION
KEGG_FOCAL_ADHESION
KEGG_PEROXISOME
KEGG_ENDOCYTOSIS
KEGG_AMINO_SUGAR_AND_NUCLEOTIDE_SUGAR_METABOLISM
KEGG_LYSOSOME
KEGG_GALACTOSE_METABOLISM
KEGG_FRUCTOSE_AND_MANNOSE_METABOLISM
KEGG_BETA_ALANINE_METABOLISM
KEGG_PENTOSE_AND_GLUCURONATE_INTERCONVERSIONS
KEGG_ASCORBATE_AND_ALDARATE_METABOLISM
KEGG_LIMONENE_AND_PINENE_DEGRADATION
KEGG_SULFUR_METABOLISM
KEGG_RNA_POLYMERASE
KEGG_CELL_CYCLE
KEGG_RNA_DEGRADATION
KEGG_PYRIMIDINE_METABOLISM
KEGG_BASAL_TRANSCRIPTION_FACTORS
KEGG_MISMATCH_REPAIR
KEGG_DNA_REPLICATION
KEGG_NUCLEOTIDE_EXCISION_REPAIR
KEGG_BASE_EXCISION_REPAIR
KEGG_NON_HOMOLOGOUS_END_JOINING
KEGG_GLYCOSAMINOGLYCAN_BIOSYNTHESIS_KERATAN_SULFATE
GSVA
1
0.5
0
−0.5
−1
Group
SI−CSC
Type
Vehicle
LDE225
Assay
Proteomics
E
GO Histone genesets
Subtype
Vehicle
LDE225
Type
FDR<0.05 and Enrichment FC>1.2
Assay
GO_REGULATION_OF_HISTONE_H2B_UBIQUITINATION
GO_HISTONE_UBIQUITINATION
GO_HISTONE_H2B_UBIQUITINATION
GO_NEGATIVE_REGULATION_OF_HISTONE_H3_K9_TRIMETHYLATION
GO_HISTONE_H3_K4_METHYLATION
GO_HISTONE_DEUBIQUITINATION
GO_HISTONE_H2A_K119_MONOUBIQUITINATION
GO_REGULATION_OF_HISTONE_H3_K36_METHYLATION
GO_HISTONE_H3_K36_METHYLATION
GO_NEGATIVE_REGULATION_OF_HISTONE_H3_K9_METHYLATION
GO_HISTONE_MONOUBIQUITINATION
GO_HISTONE_H3_S10_PHOSPHORYLATION
GO_HISTONE_MRNA_CATABOLIC_PROCESS
GO_POSITIVE_REGULATION_OF_HISTONE_PHOSPHORYLATION
GO_REGULATION_OF_HISTONE_PHOSPHORYLATION
GO_HISTONE_H3_K27_METHYLATION
GO_REGULATION_OF_HISTONE_H3_K27_METHYLATION
GO_POSITIVE_REGULATION_OF_HISTONE_H3_K27_METHYLATION
GO_REGULATION_OF_HISTONE_METHYLATION
GO_POSITIVE_REGULATION_OF_HISTONE_METHYLATION
GO_HISTONE_H3_ACETYLATION
GO_HISTONE_EXCHANGE
GO_HISTONE_METHYLATION
GO_HISTONE_H2A_UBIQUITINATION
GO_HISTONE_H4_K5_ACETYLATION
GO_HISTONE_H3_K14_ACETYLATION
GO_POSITIVE_REGULATION_OF_HISTONE_H3_K4_METHYLATION
GO_REGULATION_OF_HISTONE_H3_K4_METHYLATION
GO_HISTONE_H3_K23_ACETYLATION
GO_POSITIVE_REGULATION_OF_HISTONE_UBIQUITINATION
GO_HISTONE_H3_K36_TRIMETHYLATION
GO_HISTONE_H3_K4_TRIMETHYLATION
GO_HISTONE_H3_K36_DEMETHYLATION
GO_HISTONE_H3_K4_MONOMETHYLATION
GO_REGULATION_OF_HISTONE_DEACETYLASE_ACTIVITY
GO_HISTONE_CITRULLINATION
GSVA
1
0.5
0
−0.5
−1
Group
SI−CSC
Type
Vehicle
LDE225
Assay
Proteomics
F
GLI2
Proteomics
SOX1
Proteomics
KI67
Proteomics
ATOH1
Proteomics
SOX2
Proteomics
SI−CSC
SD−CSC
p = 0.021
p = 0.19
p = 0.0022
p = 0.057
p = 0.25
p = 0.6
p = 0.025
p = 0.7
p = 0.65
p = 0.67
Log iFOT
Vehicle
LDE225

Supplementary Figure 3. Proteomics analysis identifies differentially expressed proteins in LDE225 treated tumors. A) Principal component analysis of the 5 vehicle and 4 LDE225-treated *Ptch;p53* SI-CSC MB samples analyzed by mass spectrometry. **B**) Volcano plots of protein expression changes between vehicle vs LDE225-treated *Ptch;p53* SI-CSC MBs. Blue dots represent the down-regulated proteins and red dots represent upregulated proteins. **C**) Heatmap showing differential expression of proteins in vehicle vs LDE225 treated *Ptch;p53* SI-CSC MBs. **D)** GSVA analyses (GSVA enrichment score FC>1.2 and FDR <0.05) of vehicle vs. LDE225-treated *Ptch;p53* SI-CSC MBs showing differential enrichment of KEGG gene sets. **E)** GSVA analyses (GSVA enrichment score FC>1.2 and FDR <0.05) of vehicle vs. LDE225-treated *Ptch;p53* SI-CSC MBs showing differential enrichment of GO Histone gene sets. **F**) Expression levels of GLI2, SOX1, SOX2, ATOH1 and KI67 proteins in vehicle vs. LDE225-treated *Ptch;p53* SI-CSC and SD-CSC MBs. Box represents $\log_2$-scaled iFOT range. Central line represents the mean. P-values were calculated using two-tailed Student's t-test.

SuppFig4

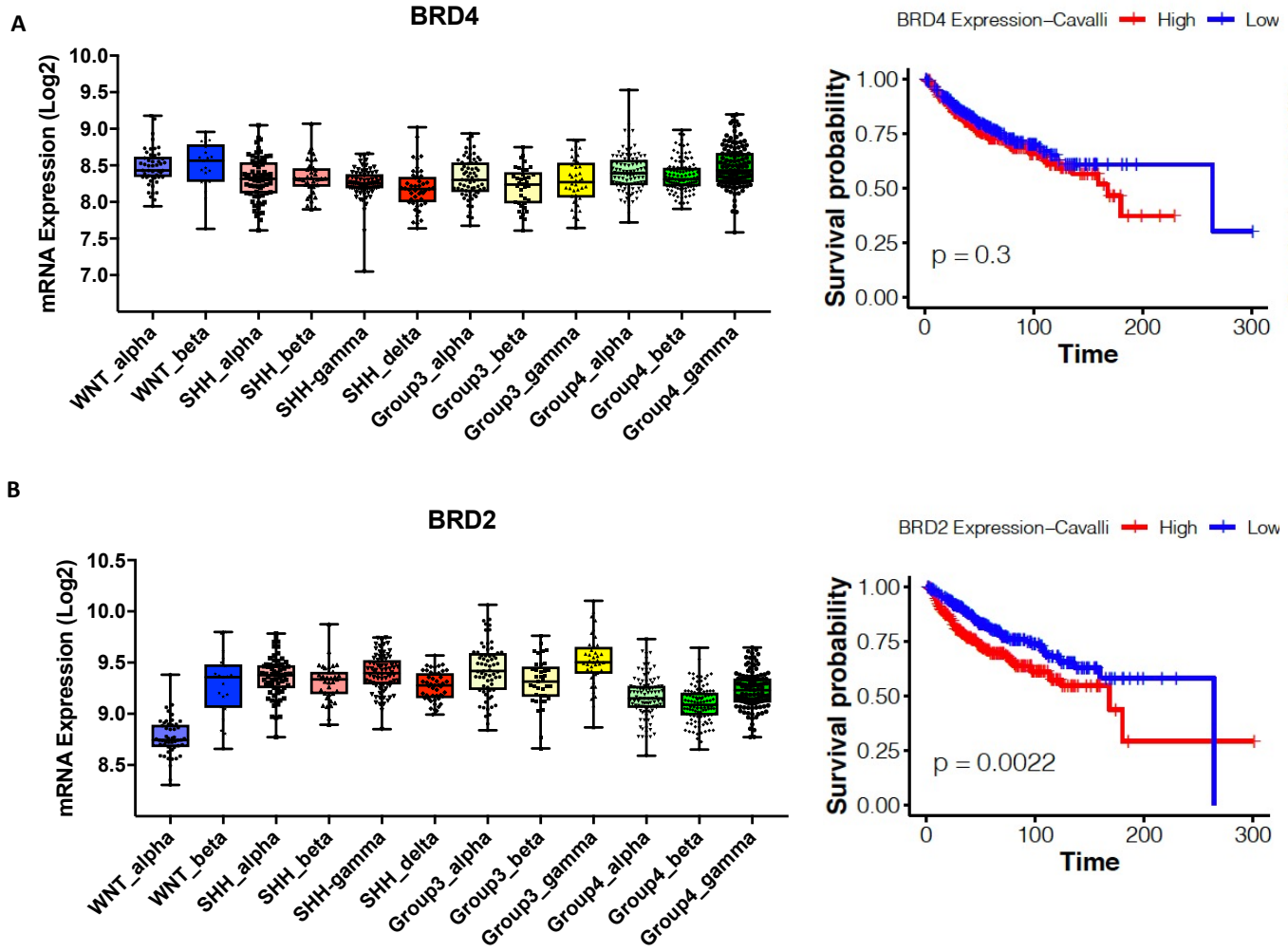

Supplementary Figure 4. Meta-analysis of GSE85217 (Cavalli *et al*) data set using GlioVis. A, B) *BRD4* and *BRD2* mRNA expression levels in different human MB molecular subtypes (left), Kaplan-Meier survival curve analyses of human MB samples by subtypes (right). High and low expression cutoff was set at the median. P-values were calculated using ordinary one way ANOVA with Tukey's multiple comparisons test. (WNT: n = 70; SHH: n = 223; Gp3: n = 144; Gp4: n = 326).

SuppFig5

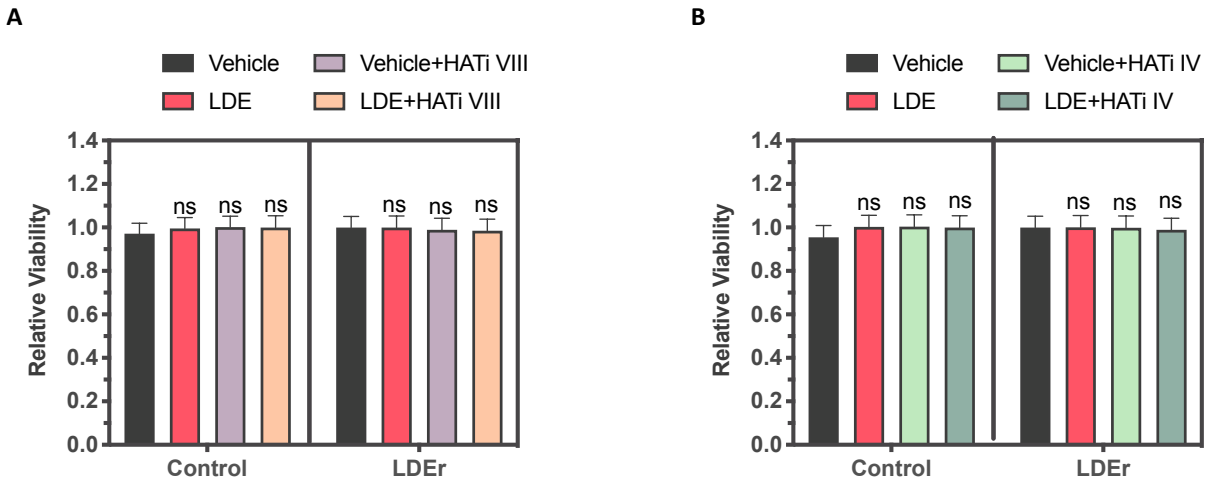

Supplementary Figure 5. HAT inhibitors are ineffective in suppressing LDE-resistant SI-CSC tumorsphere growth in vitro. A, B) Vehicle and LDE-resistant *Ptch;p53* SI-CSC tumorspheres were treated with different HAT inhibitors *in vitro*. N=3.

Supp Fig 6

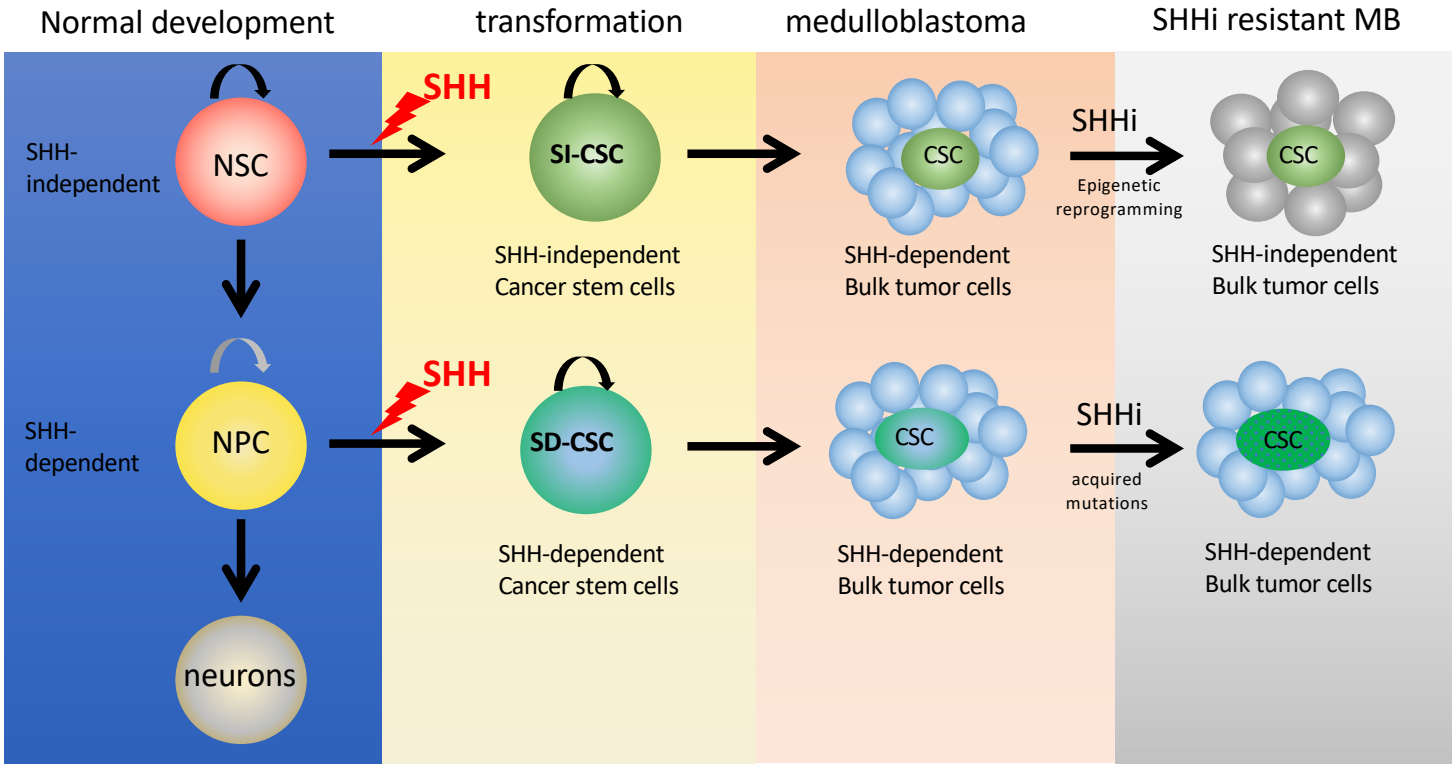

Supplementary Figure 6. A schematic summary of our working model. SHH MB can arise from transformation of either neural stem cells (NSCs, SHH-independent) or EGL neural progenitors (NPCs, SHH-dependent) in vivo. While bulk tumor cells in both tumor type depend on the SHH pathway, only the NPC-derived cancer stem cells (SD-CSC) depend on SHH signaling. SMOi treatment debulks both tumor types; however, acquired mutations within the SHH pathway occurs only in SD-CSC tumors. In SI-CSC subtype, CSCs are insensitive to SMOi and generate bulk tumor cells that deviates from normal NSC maturation through epigenetic reprogramming and generate SHH-independent progenitors/bulk tumor cells upon chronic SMOi exposure.